



Original Article

Locality effects on bifurcation paradigm of L - H transition in tokamak plasmas

Boonyarit Chatthong* and Thawatchai Onjun

*School of Manufacturing Systems and Mechanical Engineering,
Sirindhorn International Institute of Technology, Thammasat University, Khlong Luang, Pathum Thani, 12121 Thailand.*

Received: 31 January 2015; Accepted: 13 July 2015

Abstract

The locality effects on bifurcation paradigm of L - H transition phenomenon in magnetic confinement plasmas are investigated. One dimensional thermal transport equation with both neoclassical and anomalous transports effects included is considered, where a flow shear due to pressure gradient component is included as a transport suppression mechanism. Three different locally driven models for anomalous transport are considered, including a constant transport model, pressure gradient driven transport model, and critical pressure gradient threshold transport model. Local stability analysis shows that the transition occurs at a threshold flux with hysteresis nature only if ratio of anomalous strength over neoclassical transport exceeds a critical value. The depth of the hysteresis loop depends on both neoclassical and anomalous transports, as well as the suppression strength. The reduction of the heat flux required to maintain H -mode can be as low as a factor of two, which is similar to experimental evidence.

Keywords: plasma, tokamak, fusion, L - H transition, bifurcation

1. Introduction

Discovery of L - H transition is considered as one of the milestone events in nuclear fusion research (ASDEX Team, 1989). The formation of an edge transport barrier (ETB) causes a tokamak plasma to make an abrupt transition from low (L -mode) to high (H -mode) confinement modes resulting in improved performance, i.e. better energy confinement time and high plasma temperature and density (Burrell, 1994). This improvement is crucial for the success of future fusion projects, like ITER (Aymar *et al.*, 2002). It was experimentally found that an ETB formation is possible when an injected heat, regardless of heating scheme, exceeds a threshold. Theoretically, understanding the physics of L - H transition is not quite clear and still one of the open issues in fusion research (Connor *et al.*, 2000). Nevertheless, most descriptions are based somewhat on the shear of radial electric field at the onset of anomalous transport suppression and it is

believed to be a consequence of flow shear (Burrell, 1997). It is generally accepted that anomalous transport can be stabilized by the flow shear because of the breaking or a distortion of a convection cell (Biglari *et al.*, 1990). Experimental results also support that the anomalous fluxes can be reduced or quenched by a sheared flow near plasma edge (Burrell, 1997; Connor *et al.*, 2004), resulting in an L - H transition.

It is known that L - H transition phenomenon exhibits a bifurcation nature of plasmas (Malkov *et al.*, 2008). Other quantities can also exhibit this behavior such as plasma temperatures and densities, toroidal rotation and radial electric field (Wagner, 2007). The noticeable results show gradients of pressure or density profiles significantly increase at the onset of the transition. This sudden jump of gradients occurs at the plasma edge where ETB is formed. This procedure can be visually captured using an s -curve bifurcation diagram like that in the work of Malkov *et al.* (2008) where a graph of flux versus gradient has a non-monotonic behavior resulting in bifurcation regime within a certain range of heating. Figure 1 shows similar curve with addition of neoclassical regime, this will be explained in later section. In this figure, $Q_{L \rightarrow H}$ and

* Corresponding author.

Email address: boonyarit.ch@psu.ac.th

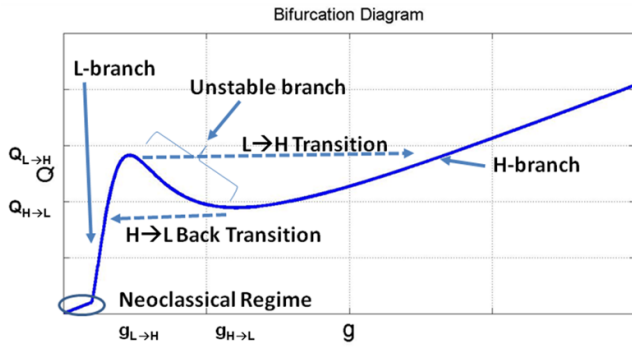


Figure 1. Basic S-curve bifurcation diagram is described for tokamak plasmas.

$Q_{H→L}$ represents heat flux at the onset of $L→H$ transition and $H→L$ back transition, respectively; while $g_{L→H}$ and $g_{H→L}$ represent their respective pressure gradients. The figure captures qualitatively possible regimes in the plasma. At low heat flux, the plasma is in the ohmic phase, which is dominated by the neoclassical transport, identified as a neoclassical regime. As heat flux increases, the anomalous effect gradually dominates the transport and the plasma reaches the L -mode regime. Once the heat flux surpasses a critical threshold, the plasma makes a sudden transition from L -mode to H -mode where anomalous transport is quenched in the transport barrier region. In the intermediate range, there exists a bifurcation regime where three equilibria are possible; two stable and one unstable. Previous works on bistable s-curve bifurcation models discussed on various characteristics of the models, which result in better understanding of the qualitative aspects as well as gaining considerable insight into $L→H$ transition physics (Chatthong *et al.*, 2015; Hinton, 1991; Hinton *et al.*, 1993; Jhang *et al.*, 2012; Lebedev *et al.*, 1997; Malkov *et al.*, 2008; Staebler *et al.*, 1996; Weymiens *et al.*, 2012). The work of Lebedev *et al.* (1997) used a one-field bifurcation model to study spatiotemporal behavior of the plasma. Malkov and Diamond later applied this concept to analyze the coupled heat and particle transport equations simultaneously and showed that with inclusion of the hyperdiffusion effect, the transition follows Maxwell's rule (Malkov *et al.*, 2008). Recently, the bifurcation concept was used to investigate toroidal effect on $L→H$ transition (Chatthong *et al.*, 2015).

This work attempts to extend the previous study on the fundamentals of $L→H$ transition as well as $H→L$ back transition in the bifurcation context. Heat transport equation including both neoclassical and anomalous effects is used. Three different assumptions for anomalous transport coefficients are considered for comparison and discussions. Note that this in-depth analysis for $L→H→L$ transitions based on bifurcation concept has never been intensively studied, especially the effect of locality. The new models for anomalous transport are locally proportional to the pressure gradient which is more realistic than the previous assumptions of having constant value throughout the plasma. In addition, it

is assumed that the anomalous transport is stabilized by the flow shear which is driven by the pressure gradient.

This paper is organized as follows: brief descriptions of bifurcation and fixed points concepts are presented in Section 2; locality effects and the resulting hysteresis are described in Section 3; and the conclusion is given in Section 4.

2. Bifurcation Concepts and Transition Points

Bifurcation concept approach for explaining an $L→H$ transition in tokamak plasma is based on the concept that plasma can be intrinsically bistable. In other words, the plasma mode can bifurcate from one regime to the other once certain criteria are satisfied. Previously, Hinton *et al.* (1993) used the Fourier transformation to identify the stability of each branch in bifurcation diagram. However, the mechanism during transition was not quite clearly explained. The attempt in this section takes different point of view, in which can be easily understood. In fact, not only the existence of three equilibrium branches within bifurcation regime is thoroughly illustrated, but the location of transitions and dynamics during transitions are also explained. This section shows that stability analysis of local plasma point can be used to describe how the plasma bifurcate to H -mode and back to L -mode in different scenarios.

This particular work focuses on a one-field transport equation, which assumes that heat and particle transport equations are completely independent from each other. This approach has shown that many important qualitative features of the $L→H$ transition can be analyzed like those discussed in the work of Lebedev *et al.* (1997). A version of heat transport equation, in slab geometry, representing the conservation of energy is of the form:

$$\partial_t p - \partial_x \left(\left[\chi_{neo} + \frac{\chi_{ano}}{1 + \alpha v_E^\beta} \right] \partial_x p \right) = H(x) \quad (1)$$

where p is the plasma pressure, χ_{neo} and χ_{ano} represent the neoclassical and anomalous transports, respectively, α is a positive constant representing the strength of the suppression, β is the mode of the suppression relating to how the turbulent convective cells are distorted by the flow shear v_E' , which is assumed to be the main mechanism for anomalous transport suppression, and $H(x)$ is the heat source of the system. This form of transport equation is improved from that discussed in the work of Malkov *et al.* (2008). It was found that the confinement improvement of H -mode is a result of transport reduction in the anomalous channel, reducing transport to a neoclassical level (Wagner, 2007). The time variation of the pressure can be written as:

$$\partial_t p = H(x) - \partial_x \left[\chi_{neo} + \frac{\chi_{ano}}{1 + \alpha g^\beta} \right] g, \quad (2)$$

where $g = -\partial_x p$ and the flow shear is assumed to be driven by the pressure gradient. Equation 2 can be integrated with

respect to x as follows:

$$\frac{\partial}{\partial t} \int p dx = \int H(x) dx - \int \frac{\partial}{\partial x} \left[\chi_{neo} + \frac{\chi_{ano}}{1 + \alpha g^\beta} \right] g dx. \quad (3)$$

with

$$w = \int p dx, \quad (4)$$

which is equal to the energy flow per surface area. Thus, $\dot{w} = \partial_t w$ represents the energy density flow of plasma within the flux surface. As a result, Equation 3 can be written as:

$$\dot{w} = Q - \left[\chi_{neo} + \frac{\chi_{ano}}{1 + \alpha g^\beta} \right] g, \quad (5)$$

where Q is the heat flux given to the plasma. This is a first-order nonlinear differential equation of the thermal transport equation. Evidently, this equation shows that only the heat flux, which is the sum of heat source function, plays a role in determining L - H transition.

Physically, Equation 5 can be treated as the time variation of the energy density, which is a function of both pressure gradient and heat flux. It is plotted in Figure 2 with each panel representing a graph of \dot{w} versus g at different values of Q . Note that the constants are arbitrarily chosen in this figure as well as in later figures. As a result, only the qualitative results should be considered. Treating a local point along the graph as an initial point, as time goes on, three different scenarios can happen. If the point lies within regions where $\dot{w} > 0$ then the plasma energy increases with time resulting in an increase of the pressure gradient (arrow to the right). On the other hand, if the point lies within regions where $\dot{w} < 0$, then the pressure gradient decreases because the plasma energy decreases with time (arrow to the left). Lastly, when the point lies where $\dot{w} = 0$, the pressure gradient does not change because the point is in equilibrium; such points are called fixed points. At a low value of Q (panel a), there exists only one stable fixed point. If Q reaches a first critical value $Q_{1^{st}crit}$ (panel b), an additional half-stable fixed point is created. At higher Q (panel c), there are three fixed points: two stable and one unstable fixed points. If Q equals a second critical value $Q_{2^{nd}crit}$ (panel d), the two fixed points on the left are combined and become a single half-stable point. If Q exceeds $Q_{2^{nd}crit}$ (panel e), the half-stable point is destroyed and there remains one stable point at a relatively high pressure gradient.

The graphical interpretation can be used to describe the dynamics of a local pressure gradient. The foundation of L - H and H - L transitions can be understood using a stability analysis approach from time evolution of the plasma profiles. One can imagine the heat flux Q as an independent variable which can be increased or decreased. Accordingly, the qualitative structure of the plasma system can potentially be changed as Q is varied. In particular, the fixed points can be destroyed or created, or their stability can also change. The critical assumption used throughout this work is emphasized here that the plasma relaxation time is sufficiently small so

that the plasma has enough time to adapt to the change of Q . Figure 3 illustrates the dynamics near bifurcation regime and identifies the transition points. In this figure, the equilibrium fixed points (both stable and unstable) as a function of heat flux are showed. This is a traditional bifurcation diagram. Essentially, what is implied here is that the pressure gradient depends non-monotonically on the heat flux. The two stable branches of the s-curve stand for low (L -branch) and high (H -branch) pressure gradients, while the other branch is physically irrelevant because it would correspond to unstable equilibrium. Based on the fixed points analysis described above, as Q is increased from zero, the plasma remains on L -branch in the bifurcation regime and jumps to H -branch when Q is greater than the second critical flux. On the other

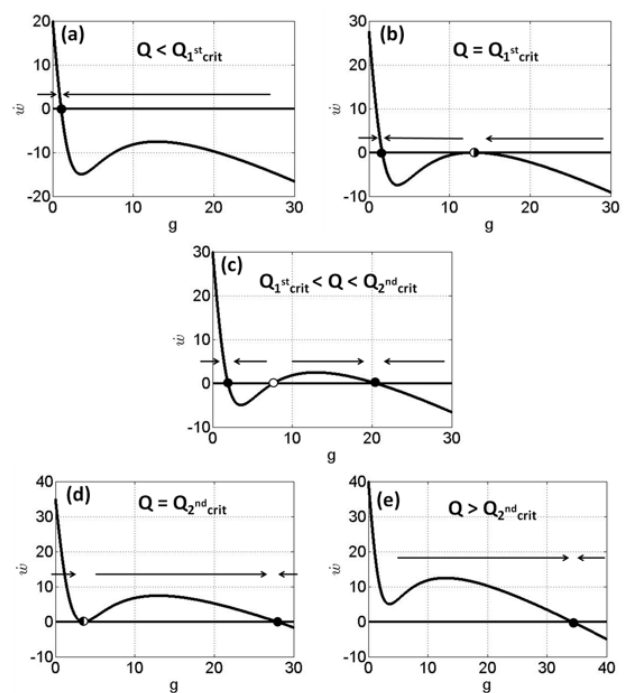


Figure 2. Fixed points for each value of heat flux and their stabilities: solid dot for stable, open dot for unstable and semi-open dot for half-stable fixed points.

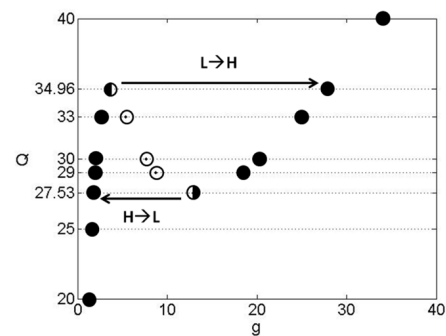


Figure 3. Bifurcation diagram constructed from fixed points illustrating 2 stable branches and 1 unstable branch with L - H and H - L transitions.

hand, when Q is decreased from high value, the plasma remains on H -branch in the bifurcation regime until Q is below the first critical flux. In fact, $Q_{2\text{ crit}}^{nd} = Q_{L \rightarrow H}$ and $Q_{1\text{ crit}}^{st} = Q_{H \rightarrow L}$. In addition, the heat flux at H - L transition is found to be lower than that of L - H transition, implying hysteresis phenomenon.

3. Locality Effects on L - H Transition and Hysteresis

This part emphasizes on the locality effects on this bifurcation description of L - H transition. In the previous works on bifurcation model (Malkov *et al.*, 2008), the neo-classical and anomalous transports are assumed to be constant. Those assumptions made the simplification suitable for analytical study but the shortcoming was that the constant transport coefficients are not physically representative. In this section, localities of plasma transports are implemented into this bifurcation picture of L - H transition. The changes and improvements are discussed.

3.1 Transition criteria

The bifurcation diagram shown in Figure 1 can be used to explain L - H transition only with non-monotonic behavior of the flux versus gradient curve. Namely, it is required that local maximum and minimum must exist to represent bifurcation regime. This requirement leads to a criterion that the ratio of anomalous over neoclassical transport coefficients has to be greater than a certain value. The criterion for constant transport coefficients was discussed in the work of Malkov *et al.* (2008) to be either 8 or 16/9 depending on the strength of shear suppression. This is a mathematical implication of the model, however it has a physical agreement where it is known that anomalous transport is one (for ion) or two (for electron) order of magnitude higher than neoclassical transport. Thus, the discussion on this paper is based on the plasma that behaves accordingly. In other words, L - H transition is always possible for the plasma with relatively high anomalous transport. Therefore, if a sufficient heat flux is provided to the system, the plasma will bifurcate to H -mode. The ratio lower than the criterion implies that the stabilization is insufficient for such a transition, which means that the plasma remains in L -mode because of no discontinuity of the gradient profile. Experimentally, if this kind of low anomalous transport can be achieved then the suppression is not even necessary and the plasma can reach high performance L -mode.

This section shows that the similar but more complicated criteria for the transition retain with more realistic models of anomalous transport used. Three different models for describing anomalous transport χ_{ano} , which is the dominant term in fusion plasma as oppose to the neoclassical term χ_{neo} , are considered. Being much less dominative, χ_{neo} is assumed to be just a constant. For the first model, the anomalous transport is assumed to be just constant, which is similar to those previous works of Hinton *et al.* (1993) and

Malkov *et al.* (2008):

$$\chi_{ano} = c_1. \quad (6)$$

For the second model, the anomalous transport is assumed to be driven by the local pressure gradient:

$$\chi_{ano} = c_2 g^m, \quad (7)$$

similar to what explored in the work of Hinton (1991) with additional parameter m representing the mode of the drive. The third model is a critical gradient model in which there exists a critical point which turns on the anomalous transport (Dimits *et al.*, 2000; Garbet *et al.*, 2004):

$$\chi_{ano} = c_3 (g - g_c) \theta (g - g_c), \quad (8)$$

where g_c is a critical gradient point, θ represents a Heaviside step function and c_i represent proportional constants. Based on these three models, the generalized form of heat transport equation at steady state is as follows:

$$Q = \begin{cases} \chi_{neo} g & , g < g_c \\ \left[\chi_{neo} + \frac{c(g - g_c)^m}{1 + \alpha(g)^\beta} \right] g & , g \geq g_c \end{cases}. \quad (9)$$

A plot of Q versus g from this equation is illustrated in Figure 1, the neoclassical regime represent the range where anomalous transport is minuscule. First of all, Equation 9 implies that $\beta > m + 1$ in order for the plot to be non-monotonic. This algebraic constraint is a limitation in which this model is applicable. Physically, this means the mode of the suppression has to be greater than the mode of anomalous transport. Algebraically, for $g \geq g_c$, the locations (g^*) of the local maximum and minimum exist where $\partial_g Q = 0$, giving relation:

$$\begin{aligned} (1 + \alpha g^{*\beta})^2 + \lambda (1 + \alpha(1 - \beta) g^{*\beta}) (g^* - g_c)^m \\ + \lambda m (1 + \alpha g^{*\beta}) g^* (g^* - g_c)^{m-1} = 0 \end{aligned} \quad (10)$$

where $\lambda = c/\chi_{neo}$. This can be rewritten to the form:

$$\lambda = \frac{(1 + \alpha g^{*\beta})^2}{(\alpha((\beta - (m + 1))g^* - (\beta - 1)g_c)g^{*\beta} - (m + 1)g^* + g_c)(g^* - g_c)^{m-1}}. \quad (11)$$

This function $\lambda(g^*)$ has a notable feature in which, for $g^* > 0$, there exist a single local minimum value. This minimum value can be calculated simply from $\partial_g \lambda = 0$. For existence of non-monotonic curve in Q versus g space, it is required that λ has to be greater than this minimum value. The first model with $m = 0$ and $g_c = 0$ yields that:

$$\lambda_1 > \lambda_{crit} = \frac{4\beta}{(1 - \beta)^2}, \quad (12)$$

which agrees with what found in the work of Malkov *et al.* (2008) with β equals to 2 and 4. The second model with $g_c = 0$ yields that:

$$\lambda_2 > \lambda_{crit} = f \alpha^{m/\beta}, \quad (13)$$

where

$$f = f(m, \beta) = \frac{(f_1 + \beta f_2 + 2f_3)^2 (2f_3)^{m-1}}{(f_1 + \beta f_2)^m [(\beta - (m+1))(f_1 + \beta f_2) - 2f_3(m+1)]^2} \quad (14)$$

$$f_1 = f_1(\beta, m) = \beta^2 + \beta(2m+1) - 2m(m+1), \quad (15)$$

$$f_2 = f_2(\beta, m) = \sqrt{\beta^2 + 2\beta(2m+1) - 4m(m+1) + 1}, \quad (16)$$

$$f_3 = f_3(\beta, m) = (\beta - m)(\beta - (m+1)). \quad (17)$$

It is analytically not possible to find the criteria for the third model ($m = 1$) because of the odd terms in Equation 11 but graphical method can be applied to show that there indeed exists a critical value like the previous two models. Before showing the graphical results, it is worth noting here that Equation 11 with $m = 1$ can be rewritten as:

$$g_c = \frac{(1 + \alpha g^{*\beta})^2}{\lambda} + \frac{2g^* - \alpha(\beta - 2)g^{*\beta+1}}{1 - \alpha(\beta - 1)g^{*\beta}}. \quad (18)$$

Apparently, the graph of g_c versus g^* has a local maximum within the applicable region. This limitation is shown as example in Figure 4 where the non-monotonic behavior of the bifurcation diagram vanishes if g_c reaches its threshold value $g_{c,th}$. Physically, g_c represents critical gradient value where the anomalous transport is turned on. Therefore, if this critical gradient is too high, then the anomalous transport will be too small relative to the neoclassical transport. Consequently, the system enters the ineffective stabilization regime or the high performance L -mode with no possibility of L - H transition. Figure 5 (top panels) also shows that as the critical gradient value is higher, the heat flux required for the transition is reduced but the gradient value at the transition is increased. This makes sense because, when the anomalous transport is reduced, it should be easier to reach the heat flux requirement ($Q_{L \rightarrow H}$). Furthermore, the bottom panels of this figure shows that the threshold of critical pressure gradient $g_{c,th}$ is increased if either the anomalous transport is increased or the neoclassical transport is decreased. In summary, this analysis shows the existence of a critical ratio of anomalous to neoclassical transport coefficients above which the L to H transition becomes a bifurcation. This critical ratio is dependent on variables m , β , the suppression constant α , as well as the critical gradient g_c .

3.2 Backward transition and hysteresis properties

It was found that H -mode plasmas can be retained even if heating power is reduced below L - H transition threshold. This hysteresis characteristic in fusion plasma has been found in various experiments and the reduction of heating power was found to be even as high as a factor of

two (Snipes *et al.*, 2000; Wagner, 2007). The bifurcation diagram, Figure 1, also captures this hysteresis loop behavior. The question of which mode the plasma resides, depends on the direction of heat ramping. If it is ramped up, the plasma makes an abrupt jump to H -mode as heat flux exceeds $Q_{L \rightarrow H}$. From H -mode plasma, if the heat flux is reduced below $Q_{H \rightarrow L}$, it transits back to L -mode. In this section, analytical study on hysteresis depth is discussed based on this bifurcation picture. Definition is given here for hysteresis depth study which consists of the heat fluxes and pressure gradients at L - H transition ($Q_{L \rightarrow H}$, $g_{L \rightarrow H}$) and back H - L transition ($Q_{H \rightarrow L}$, $g_{H \rightarrow L}$) as well as their differences (ΔQ , Δg), respectively. This

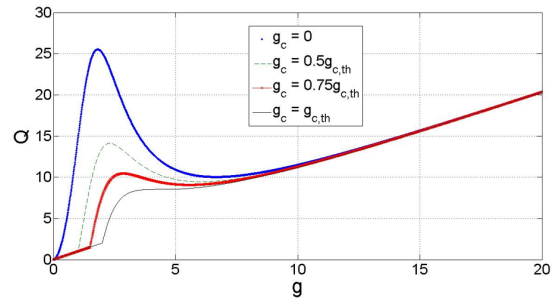


Figure 4. Bifurcation diagram at different values of critical gradient.

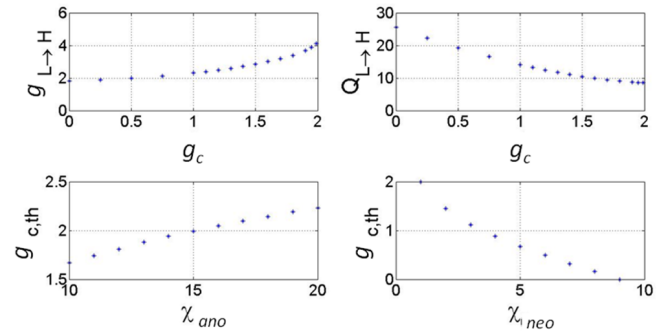


Figure 5. Effects of critical pressure gradient on the pressure gradient (top left) and threshold flux (top right) at L - H transition and effects of anomalous (bottom left) and neoclassical (bottom right) transport coefficients on the threshold limit of the critical pressure gradient.

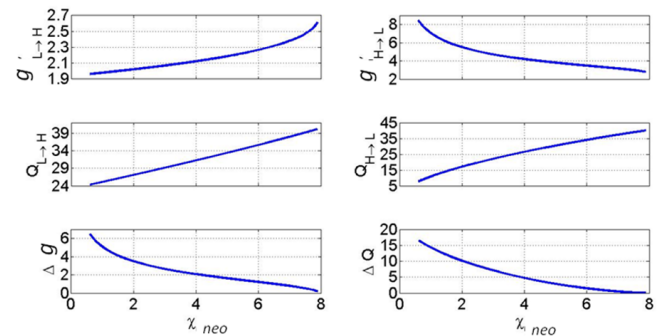


Figure 6. Hysteresis depth as a function of neoclassical transport.

part analyzes the effects of neoclassical and anomalous transports and parameter m on the hysteresis depth. This study can be used to further optimize plasma performance versus heating with respect to H -mode sustainment.

Hysteresis depth as a function of neoclassical transport is illustrated in Figure 6. First of all, the heat flux reduction ratio ($Q_{L \rightarrow H} / Q_{H \rightarrow L}$) is ranged from around 4 to 1 depending on the values of χ_{neo} . As χ_{neo} is increased, both heat flux thresholds are increased because more heat is needed to compensate the increment of the transport. The interesting part here is that the rate of thresholds increase is not the same. Consequently, it causes ΔQ to reduce non-linearly to zero or the reduction ratio becomes unity as neoclassical effect is higher. This is where the plasma reaches ineffective stabilization regime. Similarly, the difference in pressure gradient Δg is also reduced with higher neoclassical effect. It can be seen that $g_{L \rightarrow H}$ is increased while $g_{H \rightarrow L}$ is decreased.

Figure 7 shows hysteresis depth as a function of anomalous transport. The heat flux reduction ratio is ranged from around 1 to 2 as c is higher. As anomalous effect is increased, $Q_{L \rightarrow H}$ is increased almost linearly whereas $Q_{H \rightarrow L}$ is also increased but at lower rate. Both heat flux thresholds are increased because more heat is needed to compensate the increment of the transport. As a result, ΔQ is enlarged at a non-linear rate as the plasma moves away from the ineffective stabilization regime. This result tells us that at higher value of anomalous transport the hysteresis in heating becomes more prominent. Similarly, the difference in pressure gradient Δg is also increased with higher anomalous effect. It can be seen that $g_{L \rightarrow H}$ is decreased while $g_{H \rightarrow L}$ is increased.

Figure 8 shows hysteresis depth as a function of the mode m of pressure gradient driven anomalous transport for $\beta = 4$. The heat flux reduction ratio is ranged from around 2 to 1 as m is higher. As m is increased, both $Q_{L \rightarrow H}$ and $Q_{H \rightarrow L}$ are increased, the same trend as effects of c as expected. Both heat flux thresholds are increased because more heat is needed to compensate the increment of the transport. ΔQ is initially increased but its increasing rate is reduced, as the limit $m = \beta + 1$ is reached, and is eventually decreased. This is because β starts to take over at the limit. The behavior is the same in Δg and $g_{H \rightarrow L}$ while $g_{L \rightarrow H}$ keeps increasing with m .

3.3 Stability diagram

Figure 9 summarizes the discussions in this work with stability diagram. It shows the plot of ratio of anomalous over neoclassical effect λ with the heat flux Q representing different regimes in the plasma. When the ratio of anomalous over neoclassical transport is below the critical value (Equation 12 and 13), L - H transition is not possible and the plasma remains in the ineffective stabilization regime (L -mode). Above the horizontal line in the regime where the transition is possible, the mode of the plasma is determined by the heat flux. So the plasma regimes are separated into four regions: neoclassical, L -mode, H -mode and the bifurcation regime.

where the plasma can either be in L -mode or H -mode. However, the plasma can only exist in one equilibrium state which is determined from the dynamics of the heat flux variation. If the heat flux is increased from lower value, then the plasma stays in L -mode in this coexistence regime. Whereas, if the heat flux is decreased from higher value, the plasma remains in H -mode until it enters the L -mode regime. At low heat flux, the anomalous transport becomes intrinsically stabilized so the plasma is in neoclassical regime. Moreover, it can be seen that as the ratio is increased the region of bifurcation regime is also enlarged. It appears that the enlargement is nonlinear which will have significant implication on the sustainment of H -mode plasma in the high heating regime.

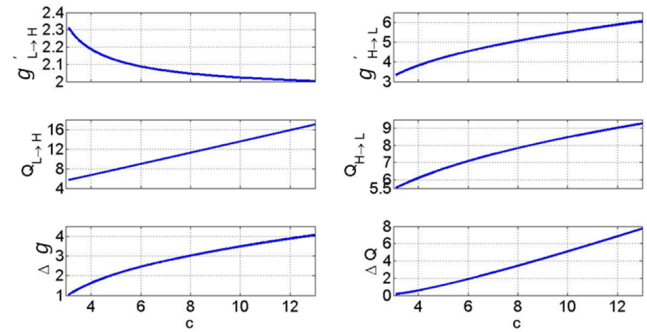


Figure 7. Hysteresis depth as a function of anomalous transport.

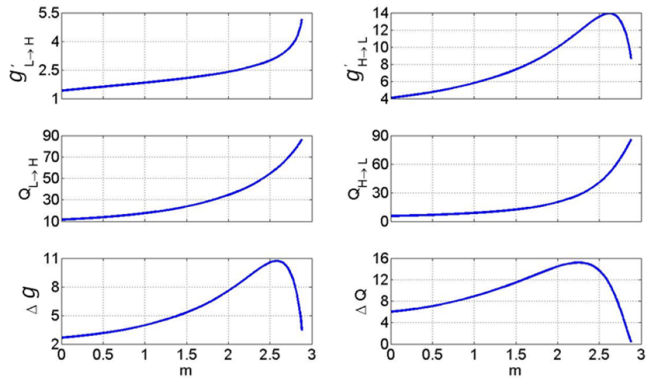


Figure 8. Hysteresis depth as a function of m .

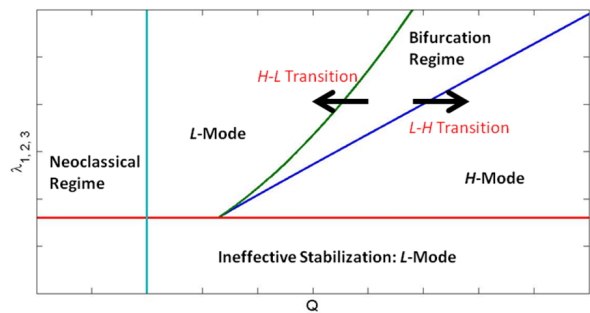


Figure 9. Stability diagram illustrating possible regimes in the plasma.

4. Conclusions

An analytical study based on bifurcation and stability of fixed points shows that at low value of heat flux the plasma is governed by neoclassical regime and at higher heat flux the anomalous transport dominates with a bifurcation nature. As a result, a sudden increase of local pressure gradient can be achieved, which exhibits the *L-H* transition. This transition is found to depend on the direction of heat ramping, where a backward *H-L* transition can occur at lower heating power than that for a forward *L-H* transition during ramping down phase, implying hysteresis phenomena. An analytical study of bifurcation shows that two conditions are necessary for plasma to make an *L-H* transition. Firstly, the ratio between anomalous and neoclassical transport coefficients must reach a critical value which is found to be a function of flow suppression and anomalous forms, in which locality effects on anomalous transport appear to stringent the requirement. This criterion persists even with more realistic choices of anomalous transport models. Secondly, the source heat flux injected into the system must be higher than a threshold. The hysteresis depth is found to be proportional to anomalous transports and inversely proportional to neoclassical transport and suppression strength except near marginal point.

Acknowledgments

This work was supported by the Commission on Higher Education (CHE) and the Thailand Research Fund (TRF) under Contract No.RSA5580041, the Royal Thai Scholarship, Bangchak Petroleum PCL, the Government Annual Research Budget through Thammasat University, and Thailand Institute of Nuclear Technology (TINT). The authors greatly thank Y. Sarazin and IRFM, CEA.

References

- ASDEX Team. 1989. The H-Mode of ASDEX. Nuclear Fusion. 29, 1959.
- Aymar, R., Barabaschi, P. and Shimomura, Y. 2002. The ITER design. Plasma Physics and Controlled Fusion. 44, 519.
- Biglari, H., Diamond, P.H. and Terry, P.W. 1990. Influence of sheared poloidal rotation on edge turbulence. Physics of Fluids B: Plasma Physics. 2, 1-4.
- Burrell, K.H. 1994. Summary of experimental progress and suggestions for future work (H mode confinement). Plasma Physics and Controlled Fusion. 36, A291.
- Burrell, K.H. 1997. Effects of $E \times B$ velocity shear and magnetic shear on turbulence and transport in magnetic confinement devices. Physics of Plasmas. 4, 1499-1518.
- Chatthong, B. and Onjun, T. 2015. Investigation of toroidal flow effects on L-H transition in tokamak plasma based on bifurcation model. Journal of Physics: Conference Series. 611, 012003.
- Chatthong, B. and Onjun, T. 2015. Study of L-H Transition and Pedestal Width Based on Two-Field Bifurcation and Fixed Point Concepts. Acta Polytechnica. 55, 215-222.
- Connor, J.W. and Wilson, H.R. 2000. A review of theories of the L-H transition. Plasma Physics and Controlled Fusion. 42, R1.
- Connor, J.W., Fukuda, T., Garbet, X., Gormezano, C., Mukhovatov, V., Wakatani, M., the ITB Database Group, the ITPA Topical Group on Transport and Internal Barrier Physics. 2004. A review of internal transport barrier physics for steady-state operation of tokamaks. Nuclear Fusion. 44, R1.
- Dimits, A.M., Bateman, G., Beer, M.A., Cohen, B.I., Dorland, W., Hammett, G.W., Kim, C., Kinsey, J.E., Kotschenreuther, M., Kritz, A.H., Lao, L.L., Mandrekas, J., Nevins, W. M., Parker, S.E., Redd, A.J., Shumaker, D.E., Sydora, R. and Weiland, J. 2000. Comparisons and physics basis of tokamak transport models and turbulence simulations. 7, 969-983.
- Garbet, X., Mantica, P., Ryter, F., Cordey, G., Imbeaux, F., Sozzi, C., Manini, A., Asp, E., Parail, V., Wolf, R. and the JET EFDA Contributors. 2004. Profile stiffness and global confinement. Plasma Physics and Controlled Fusion. 46, 1351.
- Hinton, F.L. 1991. Thermal confinement bifurcation and the L- to H-mode transition in tokamaks. Physics of Fluids B: Plasma Physics. 3, 696-704.
- Hinton, F.L. and Staebler, G.M. 1993. Particle and energy confinement bifurcation in tokamaks. Physics of Fluids B: Plasma Physics. 5, 1281-1288.
- Jhang, H., Kim, S.S. and Diamond, P.H. 2012. Role of external torque in the formation of ion thermal internal transport barriers. Physics of Plasmas. 19, 042302.
- Lebedev, V.B. and Diamond, P.H. 1997. Theory of the spatiotemporal dynamics of transport bifurcations. Physics of Plasmas. 4, 1087-1096.
- Malkov, M.A. and Diamond, P.H. 2008. Analytic theory of L→H transition, barrier structure, and hysteresis for a simple model of coupled particle and heat fluxes. Physics of Plasmas. 15, 122301.
- Snipes, J.A. and the International H-mode Threshold Database Working Group. 2000. Latest results on the H-mode threshold using the international H-mode threshold database. Plasma Physics and Controlled Fusion. 42, A299.
- Staebler, G.M., Hinton, F.L. and Wiley, J.C. 1996. Designing a VH-mode core/L-mode edge discharge. Plasma Physics and Controlled Fusion. 38, 1461.
- Wagner, F. 2007. A quarter-century of H-mode studies. Plasma Physics and Controlled Fusion. 49, B1.
- Weymiens, W., Blank, H.J.d., Hogeweyj, G.M.D. and Valenca, J.C.d. 2012. Bifurcation theory for the L-H transition in magnetically confined fusion plasmas. Physics of Plasmas. 19, 072309.